

Boundary Layer Observations in West Africa using a novel microwave radiometer

Bernhard Pospichal^{1,2}, Susanne Crewell²

¹ Meteorological Institute, University of Bonn, Germany

² Institute for Geophysics and Meteorology, University of Cologne, Germany

prepared for the special issue of "Meteorologische Zeitung"

associated with the ISARS Meeting '06

manuscript version from November 27, 2006

Corresponding author address:

Bernhard Pospichal

Institute for Geophysics and Meteorology, University of Cologne

Kerpener Str. 13, 50937 Cologne, Germany

Tel: + 49 221 4707301

Fax: + 49 221 4705161

Email: bpospich@meteo.uni-koeln.de

Abstract

Boundary layer measurements in Nangatchori, Benin, using a novel ground-based microwave profiler and additional remote-sensing instruments are being performed over the period of one full year, i.e. 2006. In this paper, the diurnal cycle of the ITD (Inter-Tropical Discontinuity) in the transition period between dry and wet season during the month of April is described in detail. Continuous observations of these phenomena in terms of temperature and humidity profiles have been achieved for the first time with a high temporal resolution of less than 15 minutes. Especially the ability of the microwave radiometer to provide high vertical resolution temperature profiles through multi-angle information gives together with meteorological tower observations detailed boundary layer information. Together with additional lidar ceilometer observations of aerosol backscatter the change of air masses, i.e. dry air masses from the north (Sahel) and moist air from the south (tropical Atlantic Ocean), which results in very sharp temperature and humidity gradients in the low troposphere, can be seen very well. The high data availability of > 85 % allows a statistical analysis of the full month in which Nangatchori is increasingly under the influence of tropical air. Thus the data set is well suited for an improved process understanding, model evaluation in a data sparse area and possibly together with additional observations the development of improved parameterizations.

Zusammenfassung:

Messungen in der atmosphärischen Grenzschicht mit einem neuartigen Mikrowellenprofiler und zusätzlichen Fernerkundungsinstrumenten werden während des gesamten Jahres 2006 in Nangatchori, Benin durchgeführt. Dieser Artikel beschreibt im Detail den Tagesgang der ITD (Innertropischen Diskontinuität) in der Übergangsphase zwischen Trockenzeit und Regenzeit während des Monats April. Erstmals gelang es, kontinuierliche Beobachtungen von Temperatur- und Feuchteprofilen mit einer zeitlichen Auflösung von weniger als 15 Minuten durchzuführen. Die Fähigkeit des Mikrowellenradiometers, Temperaturprofile in hoher vertikaler Auflösung zu liefern, erlaubt es, zusammen mit meteorologischen Messungen an einem Turm und Ceilometer-Beobachtungen, genaue Informationen über die Grenzschicht zu bekommen. Luftmassenwechsel bei Durchzug einer Front mit scharfen Temperatur- und Feuchtegradienten zwischen trockener Luft im Norden (Sahel) und feuchter Luft im Süden (tropischer Atlantik) konnten sehr gut

beobachtet werden. Die hohe Datenverfügbarkeit ($> 85\%$), erlaubt eine statistische Analyse des gesamten Monats April, in dem Nangatchori fortschreitend immer mehr unter den Einfluss der tropischen Luftmassen gelangt. Weiters ist der Datensatz sehr gut geeignet, diese Prozesse grundlegend zu verstehen, eine Validierung atmosphärischer Modelle in einer datenarmen Region durchzuführen und vielleicht zusammen mit zusätzlichen Beobachtungen verbesserte Parametrisierungen zu entwickeln.

1. Introduction

The mechanisms that influence the strength of the West African Monsoon are still not well understood. The African Monsoon Multidisciplinary Analysis (AMMA) project has been launched to get a deeper insight to this question by combining a huge number of ground-based, maritime, airborne and satellite measurements. (REDELSPERGER et al., 2006). Atmospheric humidity plays a key role in those processes that determine the strength of the monsoon. A very significant part of the water - whether liquid or as water vapor - is located in the atmospheric boundary layer. For this reason, the observation of the lowest part of the atmosphere is essential to get a comprehensive view of the monsoon.

The diurnal cycle of atmospheric processes is recognized to be a key factor for the meridional transport of humidity in West Africa. A detailed overview over the previous research is given by PARKER et al. (2005) which is briefly summarized in the following: During daytime a heat low develops over the Sahara with a pressure minimum in the afternoon. There are only weak winds in the convective boundary layer due to turbulent mixing of the atmosphere. Turbulence stops rapidly when sensible heating diminishes in the late afternoon, and the flow is able to respond to the heat-low pressure gradient force. The low level southerly flow intensifies over night and its peak moves northward. This nocturnal meridional flow is responsible for the advection of moist air in low levels further inland and is the main moisture source for summertime convection in the Sahel. In higher regions around 700 hPa there is a dry return flow. By day the low level humidity falls, as dry air from above is mixed down in the developing convective boundary layer.

Observations are rather sparse in West Africa. The radiosounding network is currently enhanced as part of AMMA, however, even then, most of the station performed soundings only two to four times a day at the main synoptic hours. In the past some campaigns, e.g. HAPEX-Sahel 1992 and Jet 2000 (THORNCROFT et al., 2003) have provided more detailed observations by aircraft, enhanced radiosoundings, pilot balloons as well as in situ surface stations. SCHRAGE et al. (2006) describe the structure of the atmosphere (temperature, humidity, and wind) for both cloudy and clear nights, using a dataset of radiosoundings in Parakou. These soundings were performed twice a day from April to October 2002. Since all these data are confined to limited time intervals PARKER et al. (2005) note the complete lack of measurements with high temporal resolution in

that region. This deficit can also not be closed through satellite observations as those measurements cannot resolve the atmospheric boundary layer.

In order to fill the gap of detailed observations in West Africa AMMA initiated the setup of the the Nangatchori site in Benin where a number of remote sensing and in-situ observations was installed. Continuously thermodynamic monitoring of the lower troposphere is performed in 2006 by a novel ground-based microwave radiometer the Humidity And Temperature PROfiler HATPRO (ROSE et al. (2005). Compared to other microwave radiometers HATPRO is available to observe high vertical resolution temperature profiles in the atmospheric boundary layer (CREWELL and LÖHNERT, 2003) in addition to the standard products IWV (integrated water vapor), LWP (cloud liquid water path), temperature and humidity profiles. To our knowledge this has been the first time that a microwave radiometer was used in West Africa for monitoring of the lower troposphere with a high temporal resolution. Additional instruments at Nangatchori include a lidar ceilometer, vertical pointing Doppler rain radar, measurements of temperature, humidity and wind on a tower in 5 levels up to 5 m, detailed in situ aerosol observations, wind profiler and ozone lidar.

This paper presents first results obtained from the combination of ground-based instruments at Nangatchori with a special focus on the novel microwave radiometer (section 2). The observations are illustrated by a case study of the diurnal cycle of the ITD in April 2006 (section 3). A first glimpse of the expected long-term potential of the observations is given by a statistical analysis for the full April where the transition from dry to wet season occurred (section 4).

2. Observations:

2.1 Measurement site

The site of Nangatchori is located 10 km south-east of Djougou (9.65° N, 1.73° E) at 415 m above mean sea level (Fig. 1). Djougou is the capital city of a province with the same name in central Benin and about 300 km north of the coastline of the Atlantic Ocean (Gulf of Guinea). This area lies in a tropical climate with a dry season between October and March and a wet season between April and September (also known as Savanna climate or tropical wet and dry climate). Temperatures rarely drop below 20°C; the extreme temperature range is 15 to 45°C.

The measurement site is surrounded by manioc fields and some shrubbery in the east of the small village of Nangatchori. The site was established in early 2005 to serve as an AMMA measurement site and for security reasons the site is permanently guarded. The University of Bonn installed one microwave profiler (HATPRO), one lidar ceilometer and one Micro Rain Radar (Fig. 2) in January 2006. These three instruments will operate in an autonomous mode over a full year until January 2007.

For a complete characterization of the atmosphere and the surface exchange processes many other instruments are located at this site. Measurements of chemical compounds of the atmosphere as well as aerosol particle observations are performed. Besides the lidar ceilometer two other instruments for optical remote sensing, one aerosol and ozone lidar, are operated in Nangatchori. Wind profile information has been gathered by Very High Frequency (VHF) and Ultra High Frequency (UHF) radars since May 2006. Furthermore, a disdrometer and some pluviometers have been installed for precipitation studies. A six meter tower for eddy correlation measurements (water vapor and CO₂ fluxes) has been constructed. It is equipped with temperature and humidity sensors as well as anemometers in different levels. The temperature sensors which were used in the case study in section 3 are located 1.2 m, 2.5 m and 4 m above ground, the data is available with a 15 minute temporal resolution. Wind direction and speed measurements were performed in four levels, later only the wind at 6 m has been used.

Although the site is safe-guarded the infrastructure to operate the various instruments without skilled operators is quite problematic due to the unreliable power supply and missing phone and internet connection. Therefore much effort had to be put into preparing the instruments for the hot and partially humid climate as well as into installing unbreakable power supplies together with reliable procedures for automatic restarting in case the power cuts exceeded 3 hours. However, up to August 2006 the data availability of the two main instruments HATPRO and ceilometer which are described in detail below has been very good (>80 %). Tab. 1 gives an overview over some instrument specifications.

2.2 Microwave radiometer HATPRO:

The microwave radiometer HATPRO (ROSE et al., 2005) continuously measures thermal emission by atmospheric components (water vapor, oxygen, liquid water) simultaneously in 14

channels distributed over two frequency bands. Seven channels are located along the high-frequency wing of the water vapor absorption line at 22.235 GHz, and another 7 channels are located along the low-frequency wing of the oxygen absorption complex around 60 GHz. Coarse profiles of water vapor and temperature can be derived from the multi-spectral measurements along these lines when viewing in zenith direction. While the IWV can be derived with a high accuracy of about 1 kg m^{-2} from the strength of the water vapor line information on the vertical distribution is limited to about two independent layers (LILJEGREN et al., 2005). For the temperature profile the situation is slightly better with a vertical resolution of about 1 km at 1 km height degrading with increasing height. Because the emission by clouds increases with frequency the liquid water path can be retrieved as well with an accuracy of about 25 g m^{-2} (LÖHNERT and CREWELL, 2003).

HATPRO is operated in zenith pointing mode most of the time giving a set of 14 brightness temperatures every 2 seconds. Statistical algorithms are used in order to retrieve atmospheric parameters from brightness temperatures. These algorithms are developed for geographic regions using radiative transfer calculations, performed on the basis of a representative long-term radiosonde data set (LÖHNERT and CREWELL, 2003). Statistical algorithms are limited for the range of atmospheric conditions for which they have been trained. Due to the lack of a reasonably good dataset of radiosondes in Western Africa the boundary layer temperature profiles as well as the humidity profiles used for this study are generated by applying a retrieval algorithm based on a 15-year radiosonde dataset of Darwin, Australia. This procedure seems reasonable since the climatic conditions in Northern Australia with marked dry and wet seasons are similar to those in central Benin. In Nangatchori, the zenith pointing mode was tilted by 20 degrees to the north to avoid direct sunlight. As a consequence, the optical path through the atmosphere is increased by 6.4 % which has been taken in to account by developing special retrieval algorithms.

The vertical resolution of the temperature profiles can be improved by performing elevation scans at relatively opaque frequencies. By assuming horizontal homogeneity of the atmosphere the observed radiation systematically originates from higher altitudes the higher the elevation angle. Since these brightness temperatures vary only slightly with elevation angle, the method requires a highly sensitive radiometer and stable radiometer. CREWELL and LÖHNERT (2006) could demonstrate HATPRO's ability for that by comparisons with radiosondes and temperature

measurements on a 100-m-mast. When using observations at six elevations between 5 and 90° the retrieval performance for the lowest 1500 m of the troposphere is significantly improved compared to zenith mode with an error <0.5 K. Therefore boundary layer scans were performed every 10 min in order to observe the evolution of night-time temperature inversions with high vertical as well as temporal resolution. The retrieval combines brightness temperatures measured at the four highest frequencies (54.94, 56.66, 57.30, and 58.00 GHz) under 5.4°, 10.2°, 19.2°, 30.2°, 42° and 90° elevation. The use of high (relatively opaque) frequencies limits the vertical information to about 1.5 km. The vertical distance of retrieved height levels is 50 m near the ground and gradually rising to 200 m in the highest levels. It should be noted that the true resolution might be worse especially for the higher levels, depending on the actual situation

Observations are possible during nearly all weather conditions. Only when precipitation reaching the instruments causes wet antennas or radoms no useful measurements can be performed. A high power dew blower is installed to remove water droplets on the radome. Auxillary measurements of air pressure, temperature and humidity are automatically performed by HATPRO. A rain detector is used to flag periods of rain, and a GPS clock is used for exact time synchronization of measurements.

2.3 Lidar Ceilometer

The Vaisala CT25K Lidar Ceilometer continuously operates in Nangatchori since January 2006. It sends out laser pulses at 905 nm and measures atmospheric backscatter with a temporal resolution of 15 seconds and a vertical resolution of 30 m (100 ft) in 250 range gates up to 7500 m (25000 ft) distance. To avoid direct sunlight during daytime the ceilometer is tilted by 20 deg to the north. This enables us to observe through the whole year with same angle even at solstice when the sun is 15 deg north of Nangatchori.

The basic purpose of this ceilometer is to detect cloud base heights. This is internally done by the Vaisala software using first a conversion of backscatter to extinction by Klett inversion and a successive threshold to detect up to three cloud layers simultaneously.

As a further application, the backscatter profiles can indicate layers of enhanced aerosol content. This is especially true during nighttime when no solar backscatter reduces receiver sensitivity and the low vertical mixing in the boundary layer leads to distinct layers of different aerosol content. An example for this gives Fig. 3 where the change of air masses at 0015 UTC can be clearly seen.

Furthermore, between 01 and 09 UTC wave disturbances can be identified from the temporal oscillations of high backscatter in about 500 m above ground.

3. Case study of diurnal cycle over Nangatchori

The average position of the ITD (Inter-Tropical discontinuity) in January and February is just north of the Guinean coast at about 7°N (Fig. 1) although single precipitation events can occur in Central and Northern Benin even at that time. The ITD marks the gradient between moist air to the south and dry air to the north. The mean wind direction is south-east in the humid air and north-east in the dry part. Around spring equinox when the sun path crosses the equator, the ITD already lies further north caused by increasing convection in the southern part and the higher solar radiation over the Sahel area. As a consequence of the larger solar input in the Sahel region, the afternoon heat low over the Sahel area becomes stronger and the temperature gradient between the hot and dry air and the humid and relatively cool air masses over the ocean becomes sharper. Along the West African coast between Nigeria and Ivory Coast the thunderstorm activity increases significantly, whereas in the Sahel zone the highest temperatures of the year can be observed. The ITD does not proceed continuously to the north; it is rather associated with pronounced “jumps” of the convergence zone and shows also strong diurnal variability.

A pronounced diurnal cycle of the ITD position with low-level moisture transport is known to play an important role for the monsoon circulation (PARKER et al., 2005). WHITEMAN et al. (1997) performed a study in the US (Southern Great Plains) where they state the importance of low-level jet moisture transport from the Gulf of Mexico to the north. Likewise, this seems to be true for the West African region. This cycle of the ITD is influenced by a large diurnal temperature range in the dry air to the north of the ITD and the nearly constant temperature at the ocean shore. As an example, analyses of mean sea-level pressure for 10/11 April (Fig. 4) show that the meridional position of the pressure minimum varies significantly over the day. It is at its southernmost point at 18 UTC and moves north during night-time. This northward retreat of the heat low is associated with an abrupt change in temperature and humidity at a given site which will be illustrated with the help of Nangatchori observations.

In the year of 2006 the northward propagation of the ITD was delayed by several weeks. Between 0 and 5°E the position of the ITD during the first and second ten-day-period of April 2006 showed an anomaly of 1.65° and 1.3° to the south (180 and 140 km), respectively¹. Associated with this feature, the region experienced unseasonably dry conditions. Towards the end of April the ITD moved north of this area and dry air masses did not extend any longer as far south as Nangatchori.

As one example we describe in the following the 24-hour period from 10 April 2006 12 UTC to 11 April 2006 12 UTC. Sunset and sunrise time for the night 10/11 April are 1803 UTC and 0545 UTC, respectively. It has to be noted that during this period no single cloud was detected over Nangatchori. The meteorological situation is described by analyses of the Global Data Assimilation System (GDAS) at NOAA Air Resources Laboratory². During daytime on 10 April a heat low at about 10°N (Fig. 4a) occurs. The dry and cloudless atmosphere is heated by the sun and temperatures in the region rise over 40°C, the maximum temperature in Niamey (Niger) being 43°C. Further south, at the coastline large convective cells are formed with afternoon rainfall, thunderstorms were observed at 17 UTC in Cotonou.

Density differences cause the cold air masses over the sea (land-sea wind system) and the outflow of convective systems to propagate inland. The northward extent of this moist air mass is not very large because of the turbulent vertical mixing in the convective boundary layer (CBL) at daytime inland. In Nangatchori, north-easterly winds which carry dry air from southern Niger and northern Nigeria could be observed between 1400 and 1800 UTC (Fig. 5b). Over the study area, a convective boundary layer is formed, and vertical mixing allows moisture to ascend to higher levels. Towards sunset an accumulation of water vapor in levels between 2 and 4 kilometers above ground could be observed (Fig. 6). The lowest atmospheric pressure at 1800 UTC over Western Africa can be found to the west of Djougou from southern Mauretania over southern Mali to Burkina Faso (Fig. 4a). The observations and the analyses show that the ITD was situated south of Djougou at this time of day.

¹ <http://www.cpc.ncep.noaa.gov/products/fews/ITCZ/itcz.shtml>

² <http://www.arl.noaa.gov/ready/amet.html>

At sunset, the north-easterly wind at the ground declines. The lower troposphere remains very dry and a sharp and shallow temperature inversion is formed over the lowest meters above the ground through strong radiative cooling. The temperature gradient measured at the tower between 1.2 and 4 meters above ground is up to 4 K (Fig. 5a), but only the very lowest part of the boundary layer is stably stratified. Already 50 meters above ground, the temperature does not change compared to afternoon values (Fig. 7). The analyzed wind field (Fig. 4b,d,f) shows that at higher levels (925 hPa, about 300 m agl) also the wind speed remains high after sunset.

Further south, the moist and relatively cool air from the ocean and the coastal region south of the ITD starts to move north. The northward propagation of the humid air starts because the turbulence diminishes rapidly in near-surface levels due to the missing sensible heating and the flow is able to respond to the pressure gradient force.

The front of cool and humid air reaches Djougou on its way north at 0015 UTC on 11 April 2006. The arrival immediately caused a removal of the shallow temperature inversion (Fig. 5a) and a sudden rise of surface pressure by 1 hPa (not shown). However, the most striking features can be seen when looking on the wind direction which changes from 0° (north) to 180° (south) from one 15 min measurement to the other (Fig. 5). The temperature and humidity profiles measured by HATPRO reveal a moist and more or less isothermally layered air mass up to 800 meters agl (Fig. 6 & 7) which reveals air from the south replacing the well-mixed dry air. This rather shallow layer has quite strong effect on the vertically integrated water vapor which rises from 10 to 16 kg m^{-2} within 20 min (Fig. 6). The meridional extent of this phenomenon cannot be determined exactly because of the lack of data from this region. However, the analyses (Fig. 4) allow the conclusion that the northernmost parts of Benin are not influenced by the cycle of the ITD on that day.

Shortly before sunrise, another drop in boundary layer temperature by 2 K at 0500 UTC in connection with a rising IWV value from 17 to 21 kg m^{-2} occurred. Starting around 5 UTC until 8 UTC the passage of wave disturbances can be identified well by the correlated oscillations of the relative humidity (Fig. 6) and the backscatter (Fig. 3). About two hours after sunrise the start of convective boundary layer formation can be seen well in the temperature profiles (Fig. 7). It takes until noon until the whole boundary layer is well-mixed. Humidity profiles show that relative

humidity below 1 km above ground reaches the highest values between 0700 and 1000 UTC. Later, the maximum of relative humidity moves higher up. The onset of north-easterly winds around 1200 UTC removes the moist air to the south-west causing the inflow of drier air masses to the area closing the daily cycle.

Though being a well-known phenomenon the diurnal cycle could be documented through a combination of different instruments with much detail (Tab. 1). The time around 10/11 April was characterized by relatively low IWV values and a rather southern position of the ITD for this time of the year. However, this feature can also be observed in other nights with higher IWV values. How representative this particular day is can only be investigated by a long-term statistical analysis, first results are given in Section 4.

4. Statistical analysis of data:

While the previous section was focused on a one-day case study, we now want to demonstrate the potential of the observations for statistical analysis. As an example we chose the month of April which encompasses transition period from dry to wet conditions at Nangatchori. During this time data availability of HATPRO temperature profiles is 83 % with 3169 boundary layer scans performed resulting in one profile every 11.3 minutes. Zenith observations providing IWV, LWP and humidity profiles are available for about 85 % of the month. For the ceilometer measured the data availability is even better with about 99 %. The reason for the discrepancy is the failure of the HATPRO instrument to restart after one specific power break which occurred on 22 April (Fig. 8a,c)

The month of April is characterized by low cloudiness, e.g. only in 11.6 % of all measurements clouds below 7 km agl were detected by the ceilometer (Fig. 8b). It has to be noted that clouds higher than this altitude or optical thin cirrus clouds (at altitudes above the freezing level at ~4000 m) can not be detected with this instrument. In the first period from 1-18 April, the cloud fraction was very low typical for the dry season, only towards the end of the month the cloud amount increased, reaching up to 40 % on some days. Clouds below 3000 m (black bars in Fig. 8b) were mainly detected during the second part of the month.

The transition to a wetter climate is even more evident in IWV (Fig. 8d) whose mean value for the whole month is 34.6 kg m^{-2} . Dry air was present in the beginning of the month which was replaced by quite humid conditions towards the end. The lowest 24-hour-mean occurred on 10 April with 18 kg m^{-2} , whereas on 30 April a mean value of 50 kg m^{-2} , e.g. more than a doubling of IWV, could be observed.

Under the dominant clear sky conditions atmospheric stability is expected to show pronounced variations between very stable (nighttime) and unstable (daytime) conditions. Therefore the presence of temperature inversions was investigated using the following definition: For a given profile, at least one level between 50 and 1500 m agl has to show a higher temperature than the lowest retrieved value at the ground. This criterium was met by 883 HATPRO temperature profiles (27.9 %). The maximum inversion strength during this period was 5.6 K/200 m which occurred on 7 April, 2330 UTC. ($28.1 \text{ }^\circ\text{C}$ at the ground, $33.7 \text{ }^\circ\text{C}$ in 200 m above ground). This was shortly before the arrival of the moist air flow from the south which reached Nangatchori less than half an hour later. Generally, every night temperature inversions could be observed with highest values very often between 2100 and 0000 UTC. The absence of strong inversions in the early morning hours before sunset where typically the strongest radiative cooling occurs can be explained by the following mechanism: The presence of dry air before midnight allows together with weak winds a more effective radiative cooling of the near surface air layer. Stronger winds and increased moisture prevent shallow temperature inversions to be formed after the passage of the nocturnal front.

With the nocturnal passage of the ITD, sharp drops in temperature associated with increasing atmospheric humidity could be observed in many nights during the transition period. To quantify these jumps, a threshold of a 3 K temperature decrease within one hour at 200 m agl was introduced. With this criterium, between 1 and 18 April, in 16 out of 18 nights this feature could be observed. The highest temperature changes (7.1 K within one hour) were detected in the nights 9/10 and 10/11 April, the mean value of temperature jumps over all 16 nights being 5 K. The mean front arrival was at 2319 UTC, the extremum values are 2034 UTC and 0220 UTC, respectively.

Regarding more closely the Figs. 8d, e, f, and g, a five day period of moister conditions (3-7 April) is replaced by drier air masses (8-12 April). The daily mean water vapor content (Fig. 8d) correlates well with observed stability and diurnal temperature range. During the drier periods the vertical temperature gradient and the diurnal temperature range (Figs. 8f and 8g) is more pronounced. The time of arrival of the nocturnal front is also related to the mean daily IWV. In the period 3-7 April, the mean front passage at Nangatchori was at 2200 UTC, whereas from 8-12 April the front arrived at 0020 UTC (not shown). One can assume that the ITD position in the evening was further south during the drier period, causing a later arrival of the front in Nangatchori. Fig. 8e gives another interesting result: In the moister period, at 18 UTC the IWV content is higher than at 06 UTC. On the drier days, this diurnal variation is reversed. It can be seen that the case study from 10/11 April in section 3 corresponds to the driest phase of the month. It is likely that the distinct low-level inflow of dry air (Fig. 6) is not as strong during moister period.

5. Conclusions and Outlook

A first investigation of the comprehensive boundary layer observations being conducted in West Africa during the AMMA campaign in 2006 has been performed. The diurnal cycle of the ITD in the transition period between dry and wet season over Nangatchori (Benin) has been analyzed in detail using a combination of ground-based remote sensing instruments operating at high temporal resolution. The microwave profiler HATPRO turns out to be an excellent mean to determine boundary layer temperature profiles as well as humidity measurements. In the future we will further improve HATPROs retrieval products. Following CREWELL and LÖHNERT (2006) composite temperature profiles from boundary layer scans and zenith observations will be derived. Because of limited available information on the atmospheric state over Africa the statistical retrieval algorithms used in this study rely on tropical observations in Australia. The enhancement of the radiosonde network in Africa as part of AMMA will enable us to further improve the retrievals. However, it should be noted that the expected improvement will be of minor nature and no significant changes to the results presented here are expected.

Further analysis will be done in particular for the wet seasons, to describe in detail the evolution of meteorological parameters in association with squall lines and thunderstorms. Additional information of vertical wind distribution will be obtained by including data from an UHF wind profiler operated in Nangatchori since May 2006. Whether the sea-breeze circulation or the outflow of large convective cells in the coastal area has an influence on the strength of the southerly low-level jet cannot be determined by only looking on measurements at one location. Therefore, future work will comprise gathering all available observations for 2006 and look for similar observations for example in the data from the Atmospheric Radiation Measurement (ARM) mobile facility in Niamey, Niger where these phenomena are likely to happen later in the season.

The comprehensive data set over a full year cycle will enable us to investigate atmospheric processes via detailed case studies but also on a statistical basis. Both approaches can also be used to evaluate the performance of atmospheric models in a data sparse region. While case studies might be more suitable to analyze whether mesoscale models are able to reproduce the small-scale variability observed, the statistical analysis enables a long-term evaluation of global models.

Acknowledgements

Based on a French initiative, AMMA was built by an international scientific group and is currently funded by a large number of agencies, especially from France, UK, US and Africa. It has been the beneficiary of a major financial contribution from the European Community's Sixth Framework Research Programme. Detailed information on scientific coordination and funding is available on the AMMA International web site <http://www.amma-international.org>. We thank Dominique Serça for providing the meteorological tower data and Eric Houngninou for the monthly inspections and data retrieval at Nangatchori. Fruitful discussions with Andreas Fink about atmospheric processes over West Africa are greatly appreciated.

6. References

Crewell, S., U. Löhnert (2006), Accuracy of boundary layer temperature profiles retrieved with multi-frequency, multi-angle microwave radiometry. *IEEE Trans. Geosci. Remote Sens.*, accepted.

Liljegren, J. C., S. A. Boukabara, K. Cady-Pereira, and S. Clough (2005): The Effect of the Half-Width of the 22-GHz Water Vapor Line on Retrievals of Temperature and Water vapor Profiles with a Twelve-Channel Microwave Radiometer”, *IEEE Trans. Geosci. Remote Sens.*, vol. 43, pp. 1102-1108, 2005.

Löhnert, U. and S. Crewell (2003): Accuracy of cloud liquid water path from ground-based microwave radiometry. Part I: Dependency on cloud model statistics and precipitation”. *Radio Sci.*, vol. 38, 8041, doi:10.1029/2002RS002654.

Parker, D. J., R. R. Burton, A. Diongue-Niang, R. J. Ellis, M. Felton, C. M. Taylor, C. D. Thorncroft, P. Bessemoulin and A. M. Tompkins (2005): The diurnal cycle of the West African monsoon circulation, *Q. J. R. Meteorol. Soc.*, 131, 2839-2860.

Redelsperger, J. L., C. D. Thorncroft, A. Diedhiou, T. Lebel, D. J. Parker, and J. Polcher (2006): African Monsoon Multidisciplinary Analysis, *Bull. Amer. Meteor. Soc.*, accepted

Rose, T., S. Crewell; U. Löhnert, C. Simmer (2005): A network suitable microwave radiometer for operational monitoring of the cloudy atmosphere. *Atmos. Res.*, 75: 183-200.

Schrage, J.M., S. Augustyn, and A. H. Fink (2006): Nocturnal stratiform cloudiness during the West African monsoon. *Meteor. Atmos. Phys.*, in press

Thorncroft, C.D., D.J. Parker, R.R. Burton, M. Diop, J.H. Ayers, H. Barjat, S. Devereau, A. Diongue, R. Dumelow, D.R. Kindred, N.M. Price, M. Saloum, C.M. Taylor, A.M. Tompkins (2003) The JET2000 Project: Aircraft Observations of the African Easterly Jet and African Easterly Waves, *Bulletin of the American Meteorological Society* , **84**, pp.337-351.

Whiteman, C.D., X. Bian, and S. Zhong: Low-Level Jet Climatology from Enhanced Rawinsonde Observations at a Site in the Southern Great Plains. *J. Appl. Met.*, **36**, 1363-1376

| Time | Coast (6°N) | Djougou (9.7°N) | Sahel (13-15°N) |
|-----------|--|--|---|
| 12-18 UTC | Deep convection, large thundery cells with rain, moist air remains in coastal area | dry convection, deep convective boundary layer water vapor of last night is lifted from the ground to higher levels | Heat low with its center to the northwest of central Benin (Mali, northern Ghana, Burkina Faso). Dry and hot northeasterly flow |
| 18-00 UTC | "dying" convective cells, moist air starts to flow northwards | Dry Sahelian air in low levels. Boundary layer remains well-mixed except for the lowest < 100 m with a shallow temperature inversion | Pressure minimum remains over the area. At 00 UTC on 11 April it can be found over northwest Nigeria. |
| 00-06 UTC | Southerly flow | Around midnight a quick jump from dry and warm air (easterly flow) to moist and relatively cool air (south-westerly flow). Stable stratification ($dT/dz \sim 0$ up to 800 m) | Pressure gradients weaken. Moist air penetrates into southern Sahel. Lowest pressure further north than at dawn. |
| 06-12 UTC | Initiation of convection | Moisture supply from south continues, gradually onset of convection and rising convective boundary layer | Start of heat low formation. Dry air flow from north-east due to stronger pressure gradients |

Figure Captions

Figure 1. Map of Benin

Figure 2. Setting of microwave radiometer HATPRO (right), lidar ceilometer (centre) and flux station (left) at the Nangatchori site in Benin.

Figure 3. Temporal development of backscatter above the Nangatchori site derived from ceilometer observations from 10 April 2006 12 UTC to 11 April 2006 12 UTC. No clouds occurred during this time interval.

Figure 4. (a), (c), and (e) show mean sea-level pressure at 18 UTC, 00 UTC and 06 UTC, respectively. (b), (d), and (f) show wind vectors and relative humidity (in %) in 925 hPa. The black diamond represents Djougou in all plots. Source: Noaa Air Resources Laboratory, FNL Archive.

Figure 5. (a) Time series of atmospheric temperature at the Nangatchori site derived close to the ground from tower observations at three different height levels (1.2, 2.5 and 4 m above ground) from 10 April 2006 12 UTC to 11 April 2006 12 UTC. (b) Time series of wind direction in 4 m above ground level for the same period.

Figure 6. Temporal development of humidity above the Nangatchori site derived from HATPRO observation from 10 April 2006 12 UTC to 11 April 2006 12 UTC. The vertical integral, e.g. the integrated water vapor (see top), reveals strong jumps at 0015 UTC and 0445 UTC.

Figure 7. Temporal development of atmospheric temperature as boundary layer profile from HATPRO observations between 10 April 2006 12 UTC and 11 April 2006 12 UTC. The superimposed measurement of wind direction (diamonds) shows that the strong mixing at the ground occurring at midnight is related to strong jump in wind direction.

Figure 8. Statistical overview of Nangatchori measurements in April 2006. (a) Data availability of Ceilometer measurements per day (in %). (b) Fraction of the day with clouds detected by

ceilometer (in %). In black lowest cloud base < 3 km agl. Note: Cloud bases higher than 7 km agl are not detected (e.g. Cirrus clouds) (c) Data availability of HATPRO zenith observations per day (in %). (d) 24-hour mean of IWV plus standard deviation. (e) Difference between IWV at 06 UTC and IWV at 18 UTC. (f) Temperature difference between ground level and 200 m above ground. Bars show extremum values in 24-hour periods. Extremum values are mean of highest and lowest 10 % of measurements (g) Diurnal temperature range measured at the ground.

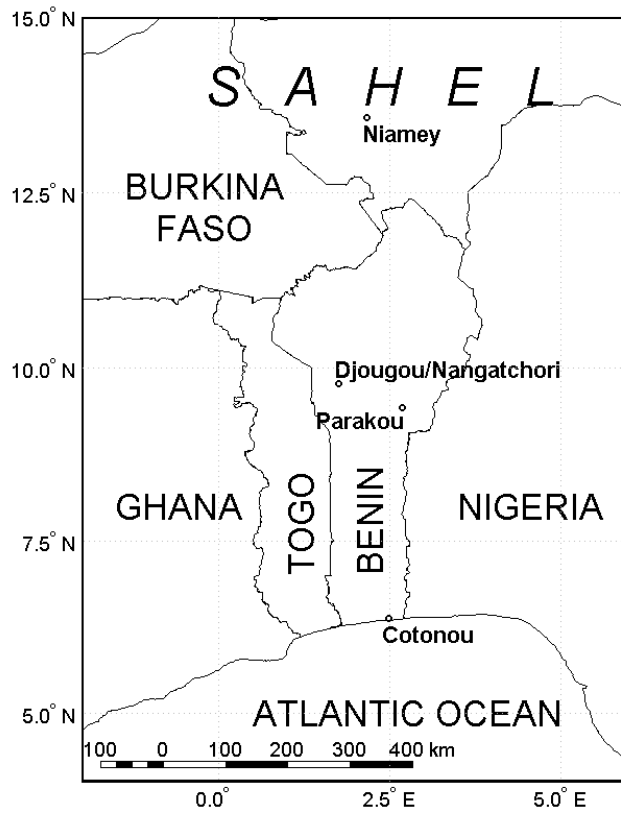


Figure 1. Map of Benin



Figure 2. Setting of microwave radiometer HATPRO (right), lidar ceilometer (centre) and flux station (left) at the Nangatchori site in Benin.

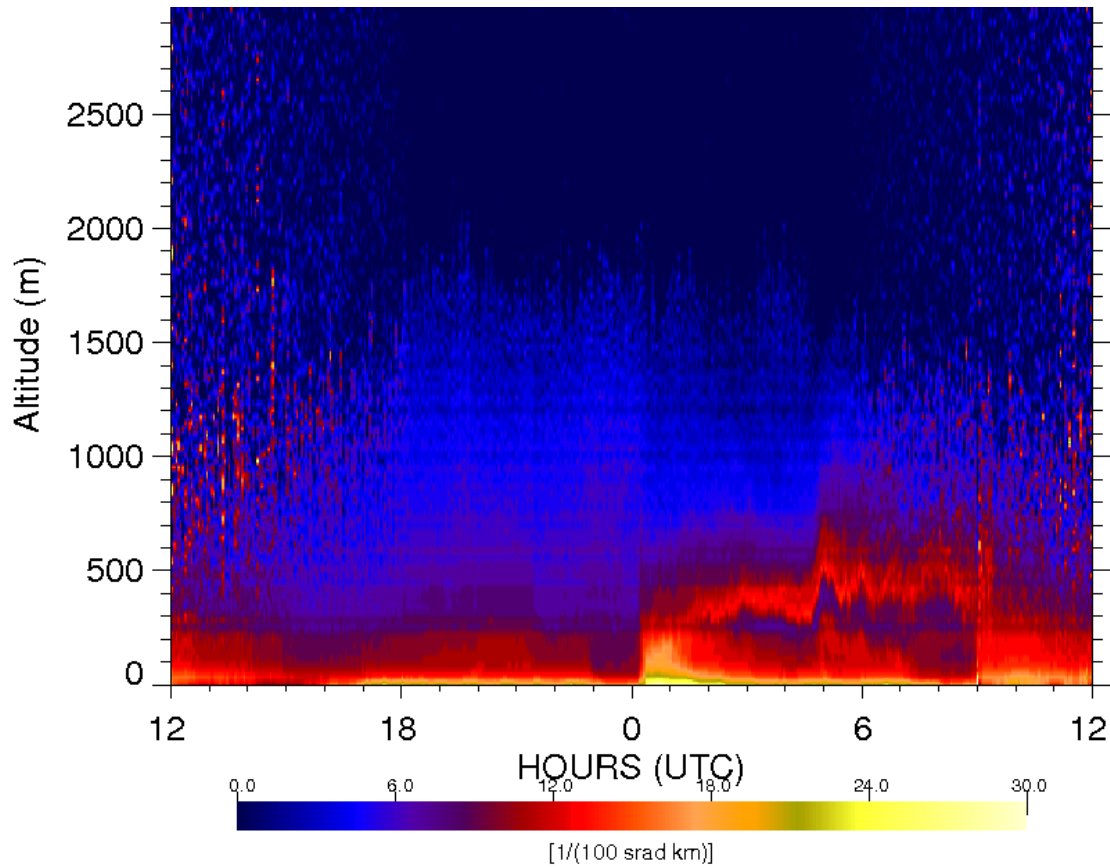


Figure 3. Temporal development of backscatter above the Nangatchori site derived from ceilometer observations from 10 April 2006 12 UTC to 11 April 2006 12 UTC. No clouds occurred during this time interval.

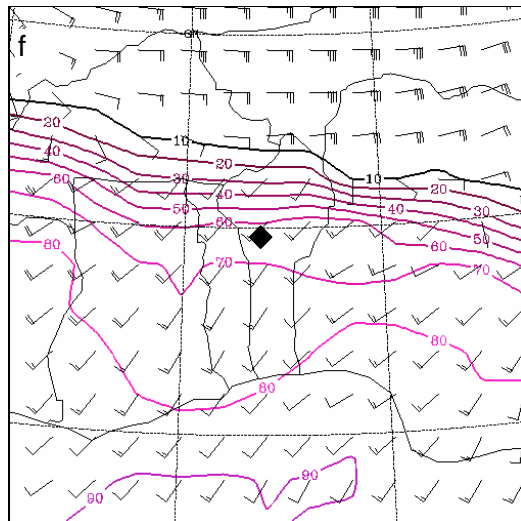
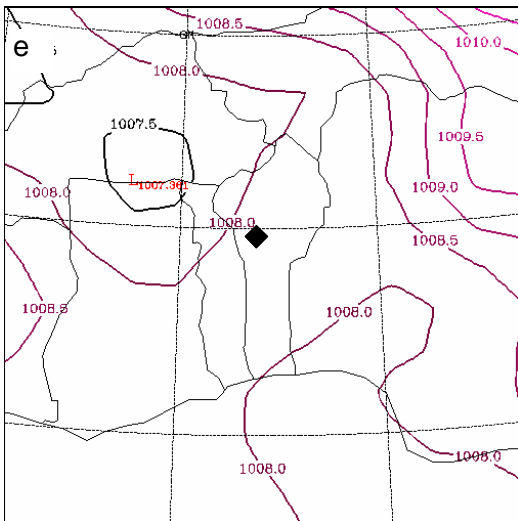
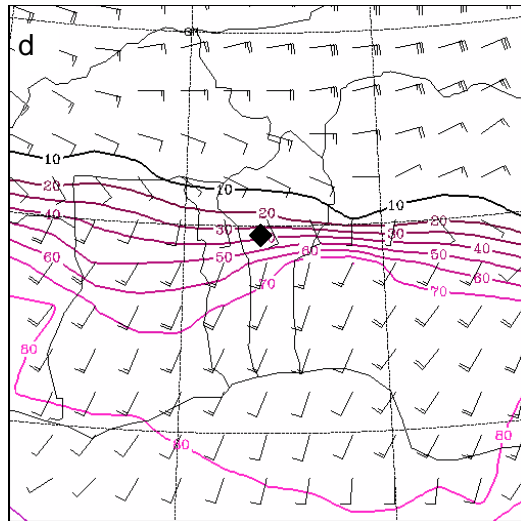
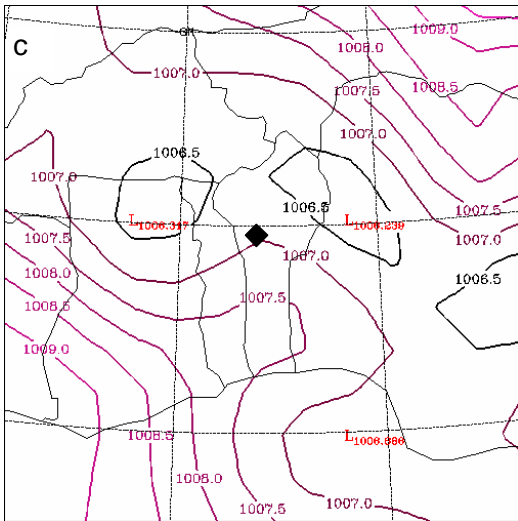
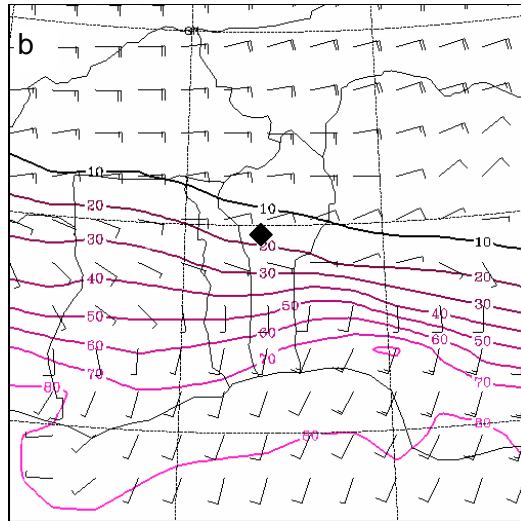
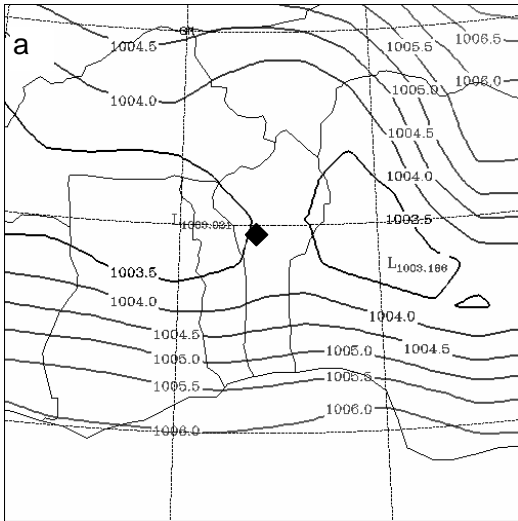


Figure 4. (a), (c), and (e) show mean sea-level pressure at 18 UTC, 00 UTC and 06 UTC, respectively. (b), (d), and (f) show wind vectors and relative humidity (in %) in 925 hPa. The black diamond represents Djougou in all plots. Source: Noaa Air Resources Laboratory, FNL Archive.

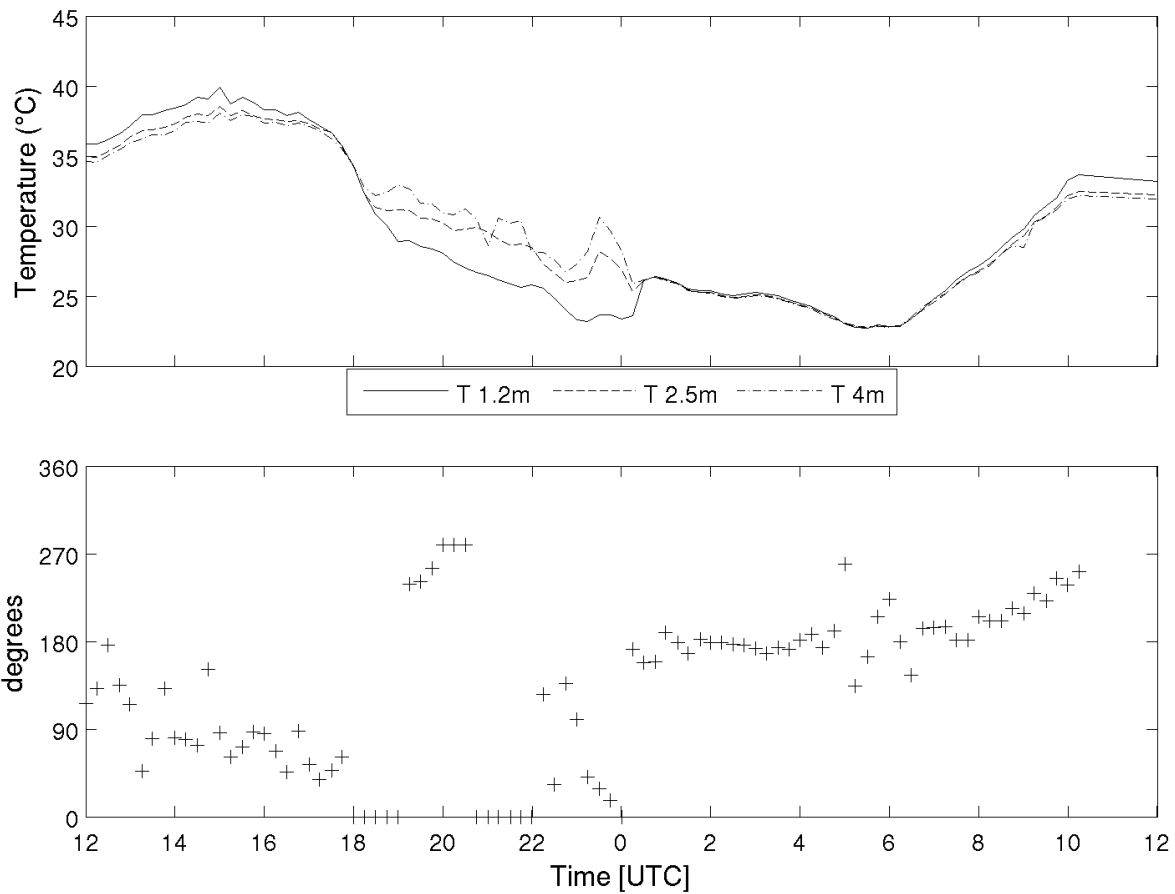


Figure 5. (a) Time series of atmospheric temperature at the Nangatchori site derived close to the ground from tower observations at three different height levels (1.2, 2.5 and 4 m above ground) from 10 April 2006 12 UTC to 11 April 2006 12 UTC. (b) Time series of wind direction in 4 m above ground level for the same period.

IWV and Relative Humidity profile Nangatchori 060410 / 060411

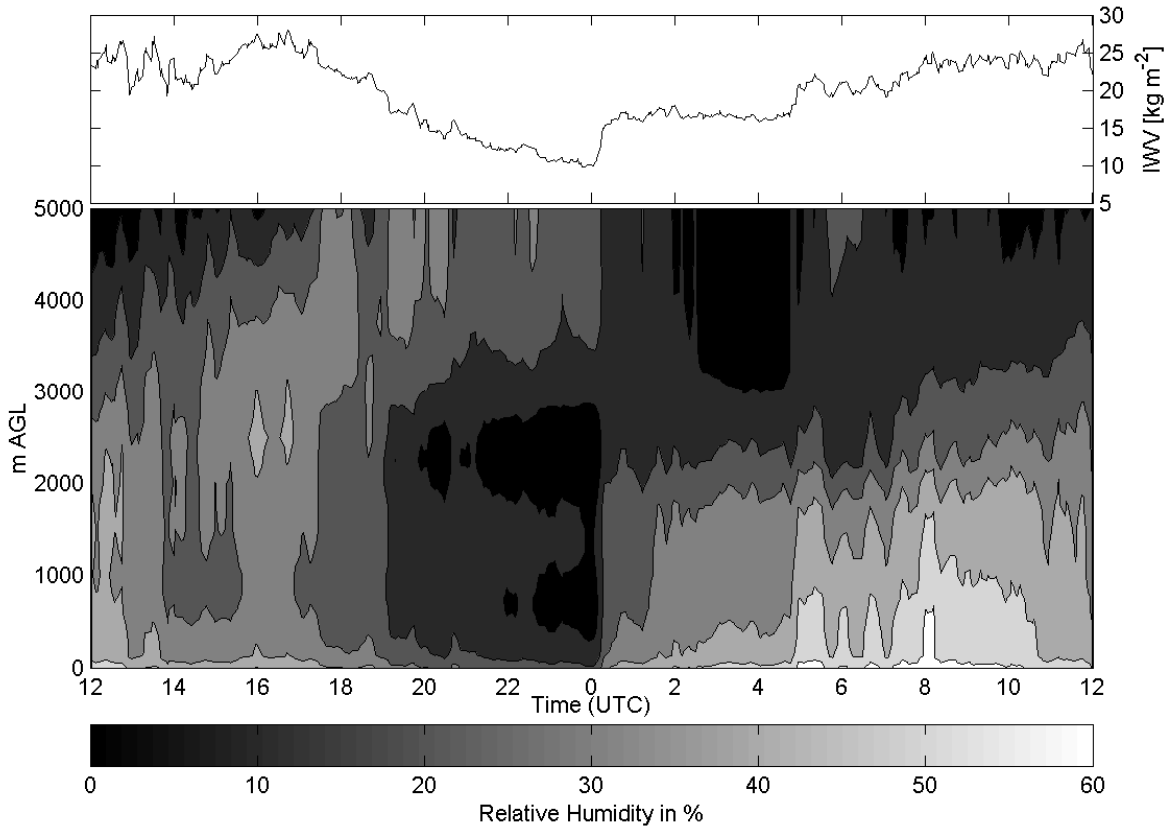


Figure 6. Temporal development of humidity above the Nangatchori site derived from HATPRO observation from 10 April 2006 12 UTC to 11 April 2006 12 UTC. The vertical integral, e.g. the integrated water vapor (see top), reveals strong jumps at 0015 UTC and 0445 UTC.

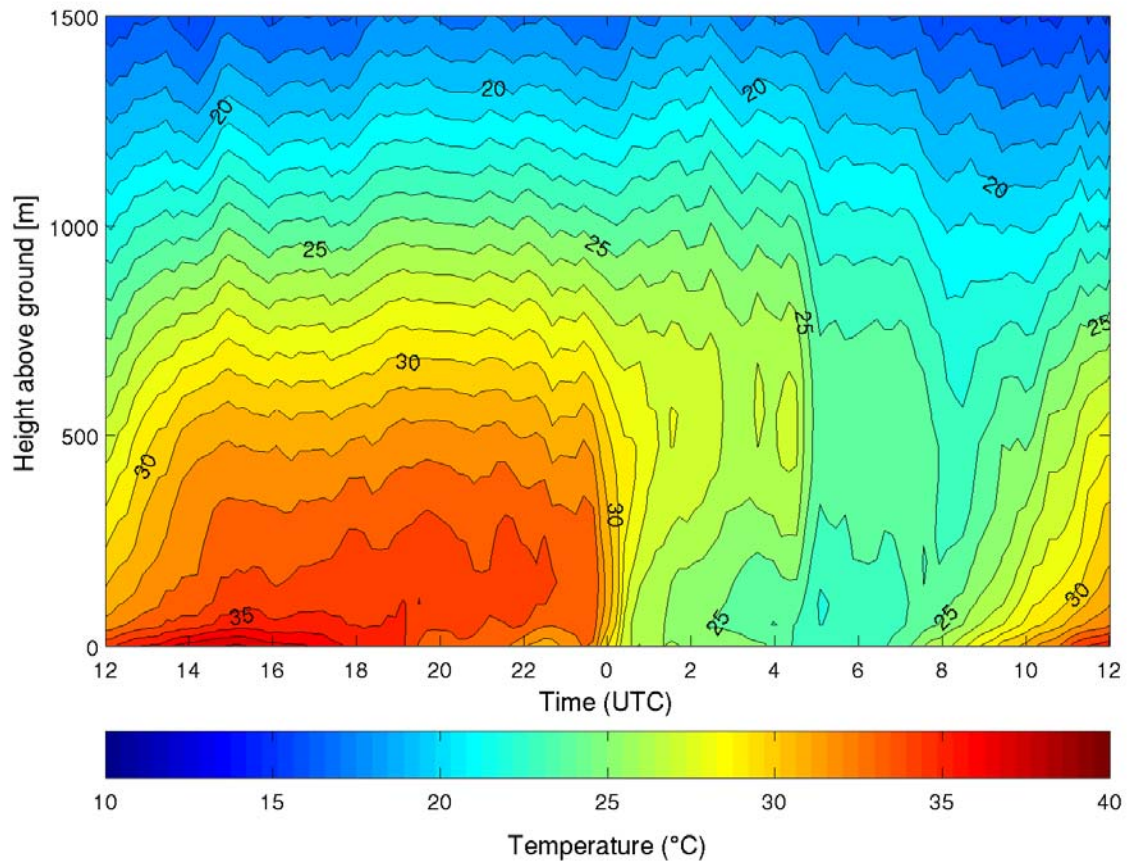


Figure 7. Temporal development of atmospheric temperature as boundary layer profile from HATPRO observations between 10 April 2006 12 UTC and 11 April 2006 12 UTC. The superimposed measurement of wind direction (diamonds) shows that the strong mixing at the ground occurring at midnight is related to strong jump in wind direction.

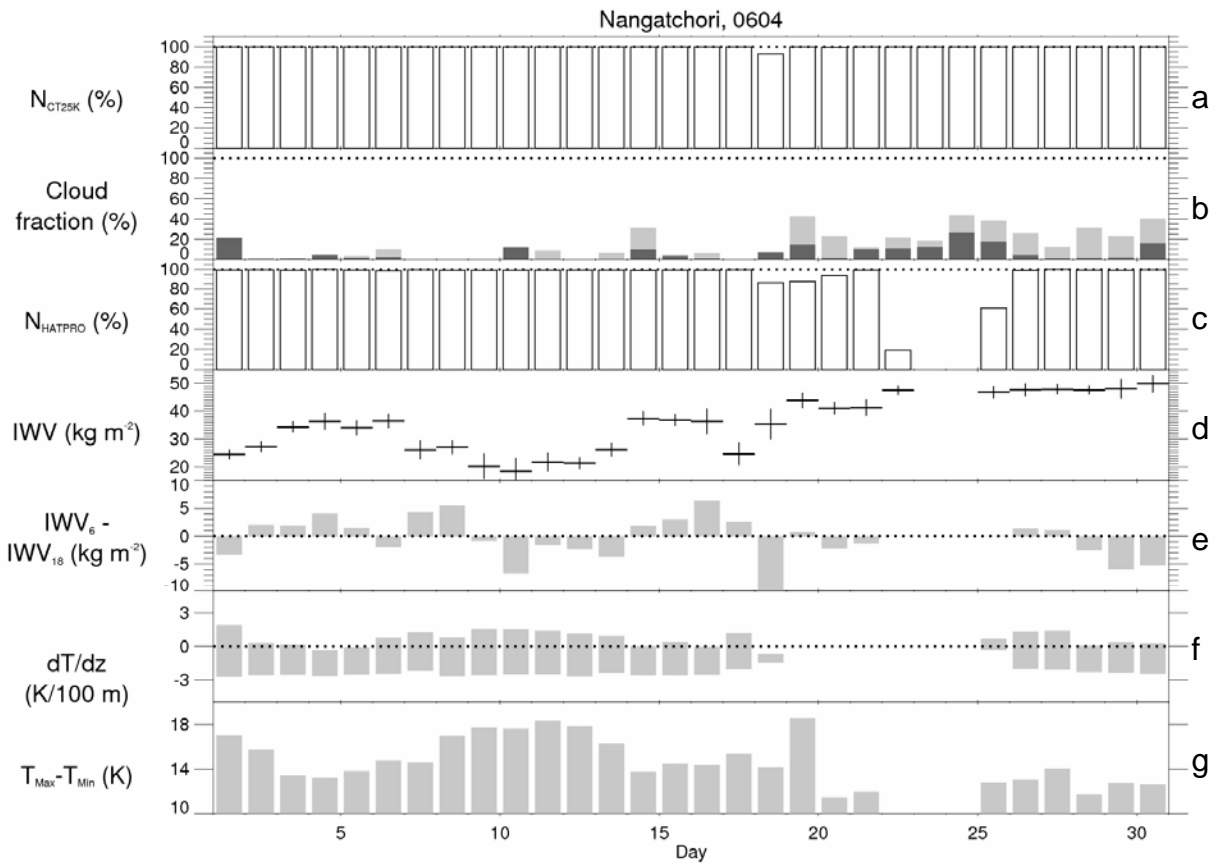


Figure 8. Statistical overview of Nangatchori measurements in April 2006. (a) Data availability of Ceilometer measurements per day (in %). (b) Fraction of the day with clouds detected by ceilometer (in %). In black lowest cloud base < 3 km agl. Note: Cloud bases higher than 7 km agl are not detected (e.g. Cirrus clouds) (c) Data availability of HATPRO zenith observations per day (in %). (d) 24-hour mean of IWV plus standard deviation. (e) Difference between IWV at 06 UTC and IWV at 18 UTC. (f) Temperature difference between ground level and 200 m above ground. Bars show extremum values in 24-hour periods. Extremum values are mean of highest and lowest 10 % of measurements (g) Diurnal temperature range measured at the ground.